Energy Advances

ROYAL SOCIETY OF CHEMISTRY

PAPER

View Article Online
View Journal | View Issue

Cite this: *Energy Adv.*, 2024, 3, 2627

Novel carbon-free innovation in centralised ammonia cracking for a sustainable hydrogen economy: the hybrid air-volt ammonia cracker (HAVAC) process

Chidozie Eluwah [ab] and Paul S. Fennell[a]

The hybrid air-volt ammonia cracker (HAVAC) represents a novel approach to centralised ammonia cracking for hydrogen production, enhancing both efficiency and scalability. This novel process integrates renewable electricity and autothermal operation to crack blue or green ammonia, achieving a high thermal efficiency of 94% to 95%. HAVAC demonstrates impressive ammonia conversion rates up to 99.4% and hydrogen yields between 84% and 99.5%, with hydrogen purity of 99.99% meeting ISO 14687:2019 standards. Key innovations include the process's flexibility to operate in three modes: 100% renewable electricity, 100% air autothermal, or a hybrid approach. This versatility optimizes energy use and adapts to varying conditions. The gas heated cracker (GHC) within HAVAC efficiently reduces energy demands by utilizing waste heat. Modelled using the Aspen Plus Simulator and validated against experimental data, HAVAC's economic analysis indicates a levelized cost of hydrogen (LCOH) between \$3.80 per kg-H_2 and \$6.00 per kg-H_2. The process's environmental benefits include reduced greenhouse gas emissions and effective NOx waste management. Future research will focus on scaling up, reducing ammonia feed cost, optimizing catalysts, and enhancing waste management. HAVAC offers substantial promise for advancing hydrogen production and supporting a sustainable, carbon-free hydrogen economy. The technical and economic data generated by this analysis will assist decision-makers and researchers in advancing the pursuit of a carbon-free hydrogen economy.

Received 30th July 2024,
Accepted 25th August 2024

DOI: 10.1039/d4ya00483c

rsc.li/energy-advances

1. Introduction

The 2023 Conference of the Parties (COP28) to the UN Framework Convention on Climate Change (UNFCCC) set an ambitious goal to reduce global greenhouse gas emissions by up to 43% by 2030, aiming to limit global warming to 1.5 °C.[1] Hydrogen is crucial to achieving this target, offering a cleaner alternative to natural gas across various applications including transportation, industry, and power generation.[2] Currently, approximately 50% of global hydrogen is produced *via* steam methane reforming (SMR).[3] As the demand for sustainable hydrogen solutions grows, there is a notable shift towards cleaner production methods to minimize carbon emissions. Recent advancements in hydrogen production technologies which include partial oxidation reforming,[4–6] auto-thermal reforming,[7–9] plasma reforming,[10–13] water electrolysis,[14–16] pyrolysis,[7,17–19] photo electrolysis,[10,16,20] sorption enhanced reforming,[2,21–24] membrane reforming,[2,25,26] integrated sorption enhanced reforming,[2,27,28] gas switching reforming,[2,29] chemical looping reforming,[2,7,30–32] chemical looping water splitting[16,32] and hydrogen production from biomass[33] *etc.* have emerged. However, these methods often produce greenhouse gases, making the integration of carbon capture and storage (CCS) essential to mitigate their environmental impact. Green hydrogen production *via* water electrolysis presents a promising pathway for sustainable energy, harnessing renewable sources to generate hydrogen with minimal environmental impact. Despite its potential, water electrolysis faces significant challenges that hinder its widespread adoption. Key issues include improving operating density, enhancing system efficiency, and addressing high-pressure storage requirements, which can reach up to 70 MPa.[14] While advanced hydrogen production technologies continue to evolve, substantial obstacles remain in the areas of hydrogen storage and transportation. These challenges are critical barriers to the development of a viable hydrogen economy, underscoring the need for ongoing research and innovation to address these issues effectively. Additionally, hydrogen's low volumetric energy density (9.9 MJ m^{-3}) and the associated storage challenges require pressurization to up to 68.9 MPa or liquefaction.[34,35] Storage materials also face issues such as hydrogen embrittlement.[36,37] Transportation options include gaseous hydrogen in trucks (up to 400 kg), cryogenic

[a] *Department of Chemical Engineering, Imperial College London, South Kensington Campus, London SW7 2AZ, UK*
[b] *Unconventional Resource Production Department, Saudi Arabian Oil Company, Saudi Arabia*

liquid hydrogen (up to 4000 kg per truck), or high-pressure pipelines (up to 100 000 kg h^{-1}).[10,38] Each method presents challenges related to high costs, energy demands, and safety risks.[10,39,40] To address storage and transportation issues, ammonia emerges as a viable hydrogen carrier due to its high hydrogen gravimetric density (17.8% by weight) and superior volumetric hydrogen density (123 kg-H_2 per m^3 at 1 MPa) compared to other storage systems such as metal hydrides (25 kg-H_2 per m^3), liquefied hydrogen (71 kg-H_2 per m^3) or methanol (99 kg-H_2 per m^3).[41,42] Other hydrogen carriers which are being studied include liquid organic hydrogen carriers (LOHCs) and boranes.[43]

Studies by the international renewable energy agency (IRENA)[44] highlight ammonia's economic advantages for long-distance transport due to low conversion costs and minimal impact of distance. Conversely, pipelines are more cost-effective for shorter distances, while liquid hydrogen and liquid organic hydrogen carriers (LOHCs) face challenges related to energy requirements and scalability.[43] Ammonia storage and transportation can utilize existing robust storage and distribution infrastructure, well-established regulation and a traceable safety record in the industry for the last 75 years.[41,45]

Ammonia cracking, used primarily in industrial processes for hydrogen production, is mainly in small-scale applications (1 to 1500 kg H_2 per day) used in metallurgical processes.[46] Significant projects are underway, including Siemens' feasibility studies and collaborations such as Proton Ventures BV's planned cracking of 3.7 million tonnes of ammonia annually.[47–50] Despite progress, there are currently no large-scale ammonia cracking plants producing fuel cell-grade hydrogen at hundreds of tons per day.[41,51] These initiatives highlight ammonia's pivotal role in future energy systems and emphasize the imperative for ongoing research aimed at optimizing both ammonia synthesis and cracking efficiencies to optimize transportation economics while advancing economic viability and sustainability. Ammonia cracking plant can either be centralised, or decentralised, plant. Centralised ammonia cracking plant concepts allow blue or green ammonia to be transported to a large cracking plant where the hydrogen produced can be distributed through the national gas network grid to homes for domestic cooking and heating or to fuel stations for fuel cell vehicles. In decentralised ammonia cracking plants, ammonia is transported to point of use and cracked onsite for fuelling stations, chemical industry or remote applications.[41,52,53]

To advance industrial-scale hydrogen production from ammonia decomposition, research has concentrated on several key areas: catalyst types, heat sources, reactor design, and hydrogen purification processes.[54] Catalytic ammonia decomposition primarily employs transition metal catalysts such as nickel (Ni), ruthenium (Ru), cobalt–iron (Co–Fe), and iron (Fe), often supported on inorganic oxides and enhanced with alkaline promoters.[55] While Ni-based catalysts are effective at high temperatures, Ru is noted for its superior catalytic activity due to its optimal metal–nitrogen binding energy. However, Ru's high cost poses challenges for large-scale industrial application.[56–65] Research efforts are increasingly directed towards optimizing non-noble metal catalysts and exploring novel formulations, such as lithium imide–amide and sodium imide–amide, to enhance catalytic performance and reduce decomposition temperatures.[64,66–72]

The ammonia decomposition process is endothermic, necessitating the application of heat. Various methods have been investigated to supply the required activation energy, including thermal decomposition using external fuels,[73–76] electric current,[77–82] plasma,[55,83–85] and solar energy.[55,86,87] Additionally, methods such as decomposition coupled with other reactions,[55,88,89] electrolysis of liquid ammonia,[55,90] and photocatalysis in gaseous or aqueous media[55,91,92] have been explored. Plasma-driven ammonia cracking, while achieving rapid decomposition through high-energy electrons, requires carrier gases like argon (Ar) or nitrogen (N_2) and suffers from low ammonia concentration in the feedstock, limiting hydrogen productivity.[55,83–85] Ammonia electrolysis can occur in aqueous or non-aqueous electrolytes. Aqueous electrolysis utilizes alkaline conditions for ammonia oxidation, producing hydrogen at room temperature but faces challenges such as corrosive environments and low ammonia solubility.[55,90] Non-aqueous electrolytes, using liquid ammonia as a solvent with ammonium salts, offer higher ionic conductivity and stability but require specialized handling.[55,90] Photocatalytic ammonia decomposition employs semiconductor photocatalysts like TiO_2 under light irradiation to produce hydrogen at ambient temperatures. Despite its potential, photocatalysis struggles with low efficiency and the production of undesired byproducts like nitrogen oxides, necessitating further catalyst development for practical industrial applications.[55,91,92] Ammonia reforming combines ammonia oxidation with its decomposition to sustain the endothermic cracking reaction. This process requires efficient catalysts and robust heat management systems to optimize hydrogen production and effectively manage exhaust gases.[55,93–97] Continued research and development in these areas are crucial for improving efficiency and scalability in ammonia-based hydrogen production technologies.

Makhloufi Camel *et al.*[41] conducted a techno-economic analysis of large-scale hydrogen production using a fuel gas-fired ammonia cracker and cryogenic separation. While this method achieved a thermal efficiency of 68.5% and a lower LCOH of 4.83 Euro per kg-H_2, significant issues include the reliance on carbon-based fuel gas, which presents environmental concerns, and overall low process thermal efficiency. These factors may impact the sustainability and economic viability of the process. Nasharuddin *et al.*[52] performed a techno-economic evaluation of decentralized (500 kg day^{-1}) and centralized (1000 tonnes day^{-1}) ammonia cracker processes. While the centralized process showed technical and economic viability with a conversion of 94% and an LCOH of 5.50 USD per kg-H_2, the decentralized plant was deemed economically unfeasible. The primary challenge lies in balancing scalability, economic feasibility, and the high dependency on ammonia feedstock costs. The Rencat Company[55] commercialized a technology for low-cost, high-purity hydrogen production from ammonia, combining catalytic decomposition and oxidation in a multi-functional reactor. Despite its innovative approach, challenges

include the integration of combustion and catalytic decomposition processes, which may complicate reactor design and operation. The need for separate channels for combustion and catalytic processes could impact the efficiency and cost of the technology. Lee Jaewon *et al.*[82] investigated an electromagnetic induction heating metallic monolith reactor process utilizing renewable electricity. Although this approach achieved 90% ammonia conversion and a notable exergy efficiency of 54.21%, challenges include the high levelized cost of hydrogen (LCOH), which was calculated as 6.98 USD per kg-H_2 for 150 N m^3 h^{-1} and 5.33 USD per kg-H_2 for 500 N m^3 h^{-1}. Additionally, the process relies heavily on low-cost renewable electricity, and 10% of the ammonia remains unreacted, impacting overall efficiency and cost-effectiveness. Sijan Devkota *et al.*[76,98] used Aspen Plus and MATLAB to model a multi-catalytic packed bed reactor with intermediate heating. Despite achieving nearly equilibrium ammonia conversion (97.21%) and a high process thermal efficiency of 79%, the single bed system only reaches 35% conversion at 500 °C and 9 barg. This method's challenge lies in the need for a complex multi-bed arrangement and intermediate heating, which may complicate scaling and operational costs. The calculated LCOH of 6.05 USD per kg-H_2 further underscores the economic challenges associated with ammonia feedstock costs. Kim J. H. *et al.*[99] explored a micro-reforming system for hydrogen production through the combustion and reforming of ammonia (NH_3). While the system achieved an NH_3 conversion rate of 97.0% and an H_2 production rate of 5.4 W, key challenges include maintaining a high overall system efficiency of only 10.4% and managing NOx emissions at 158 ppm. The system's design for effective heat transfer and fuel-equivalence ratio control remains complex and may limit scalability. Valentina *et al.*[100] demonstrated the use of a hydrogen perm-selective Pd-alloy membrane in a laboratory setting, achieving complete ammonia conversion at temperatures above 425 °C. Although hydrogen recovery exceeded 92.4%, challenges include the high cost and complexity of Pd-alloy membranes and maintaining efficient operation at elevated temperatures. These factors may limit practical industrial application and scalability.

This paper introduces the hybrid air-volt ammonia cracker (HAVAC), a novel solution designed to address several gaps identified in current ammonia cracking technologies for large-scale hydrogen production. Despite significant advancements in ammonia decomposition, several challenges remain unresolved, including enhancing process efficiency, increasing operational flexibility, producing fuel cell-grade hydrogen, reducing operational costs, and scaling production to meet growing hydrogen demands.

By overcoming these obstacles, the HAVAC is positioned to accelerate the adoption of ammonia as a viable hydrogen carrier. This advancement supports global efforts toward a low-carbon economy by providing a reliable, efficient, and cost-effective method for large-scale hydrogen production.

The novelties of HAVAC process include:

(1) The process cracks (decomposes) either blue or green ammonia optimally into fuel cell grade quality hydrogen by utilizing renewable electricity and/or air (autothermal).

(2) The process can operate between 0–100% using renewable electricity.

(3) The process can operate between 0–100% using air (autothermal).

(4) A process thermal efficiency of between 94–95% is achievable which is above current state of art.

(5) Unique process configuration.

2. Methodology

2.1 Process description

Fig. 1 is a process flow diagram. Up to 1000 tonnes day^{-1} of liquid ammonia pressurized to 1000 kPa and stored at atmospheric temperature of 20 °C is pumped through the Evaporator Exchanger, HEX-1 where the liquid ammonia is vaporized and heated to a temperature of 25 °C at a pressure of 800 kPa using the hot product gas at a temperature of 225–390 °C (the temperature depends if air autothermal operation or using renewable electricity) from the outlet of the gas heated cracker (GHC). The ammonia gas is routed through a GHC where a percentage of the feed ammonia is cracked into hydrogen and nitrogen using the hot product gas at temperature of 600–700 °C (the temperature depends on whether air autothermal operation or renewable electricity is used) from the novel hybrid air-volt cracker as the heat source. The gas heated cracker is a monolithic metallic shell and multi-tubular-multi-pass type reactor to maximize the heat transfer. The product gas from the gas heated cracker is either mixed with lean-air (air that most of the nitrogen has been removed using a nitrogen membrane package) or routed directly to the novel hybrid air-volt ammonia cracker.

When utilising renewable energy, the process is heated by electromagnetic inductive heating to 700 °C by applying an AC current through a copper coil wrapped round 410 stainless tubes. During periods of high renewable electricity cost, or low/unavailable renewable electricity, the cracker reactor operates autothermally using NH_3 as the fuel. The ammonia cracking section consists of 15–22 commercially available 410 stainless steel tubes internally coated with ruthenium catalyst. The intimate contact between the electrical heat source and the catalyst enables energy to be supplied directly to the catalytic sites, removing thermal limitations and providing well-defined control of the reaction front. 410 stainless steel tube was selected because of its very high electromagnetic properties (containing between 83–85% Iron content which provides magnetic properties). The reactor is thermally and electrically insulated.

Both the gas heated cracker and the hybrid air-volt ammonia cracker can be loaded with any optimal ammonia cracking catalyst such as ruthenium, lithium imide-amide or any other ammonia cracking catalyst. The process can uniquely operate in the below three operating modes:

- 100% renewable electricity operation at periods of surplus availability and low cost
- 100% ammonia–air mixture (autothermal) operation

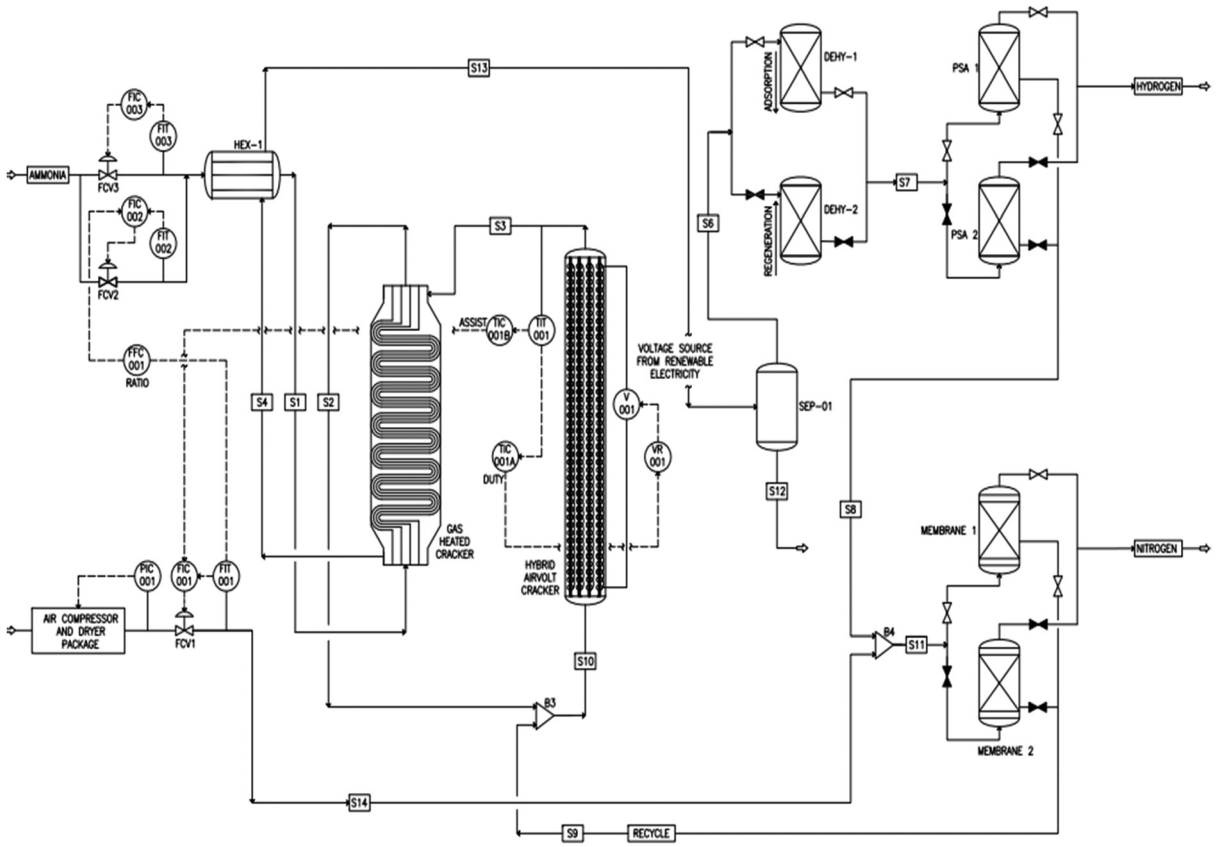

Fig. 1 Process flow diagram of novel hybrid air-volt ammonia cracker (HAVAC) process.

• Simultaneous use of both renewable electricity and ammonia–air mixture

The product gas is cooled, treated, dehydrated and purified using separator, molecular sieve and pressure swing adsorption units to produce fuel cell grade hydrogen quality as per ISO 14687:2019. NOx produced during the ammonia combustion is removed through an integrated dehydration and adsorption molecular sieve beds.

2.2 Process control system

Pressure, temperature and flowrate needs to be controlled and monitored as per Fig. 1 to operate the process optimally. Controllers like FIC-003, PIC-001, Duty TIC-001A, and Assist TIC-001B collaborate to ensure precise control. The feed forward Ratio Controller, FFC-001 calculates ammonia fuel quantity required based on stoichiometric ratio of ammonia and air. Appendix A shows the detailed process control strategy of the novel process. The hybrid air-volt cracker is the main heat supply of the process utilizing duty and assist controller concept and the principle of cascade control, feed-forward, feed-back and ratio controller system to ensure that deviations and upsets are managed properly.

2.3 Process modelling and simulation

A steady state thermodynamic equilibrium and kinetic model was developed using ASPEN Plus to model and evaluate the novel process based on a 1-D heterogenous reactor model, adopting the rate kinetics model developed by Temkin–Phyzev which has been accurately used in several other works to fit experimental conversion rate for ammonia decomposition reactions.[41,56,98,101] For high temperature range of 400 °C to 750 °C, the reaction is not limited by equilibrium,[98] and the rate reaction can be represented with a power law as shown in eqn (1) and (2).

$$NH_3 \leftrightarrow 0.5N_2 + 1.5H_2 \quad (R1)$$

Table 1 System and operating specifications for novel HAVAC process

Parameter	Value	Units
Gas heated cracker (GHC)		
Number of reactors	1 × 100%	—
Reactor pressure	800	kPa
Reactor outlet temperature	225–390	°C
Reactor tube diameter	0.09	m
Tube length	8.5	m
Number of tubes	260–400	—
Hybrid air-volt cracker		
Number of reactors	1 × 100%	—
Reactor pressure	800	kPa
Reactor outlet temperature	600–700	°C
Tube diameter	0.09	m
Tube length	7	m
Number of tubes	6–22	
Kinetic order	0.27	Ref. 98 and 101
Activation energy	117 kJ mol^{-1}	Ref. 98 and 101
Pre-exponential constant	6×10^8 s^{-1}	Ref. 98 and 101

Table 2 Ammonia combustion kinetics[64–66]

Reaction	Reaction rate expression	Pre-exponent	Activation energy (kJ mol^{-1})
$NH_3 + 1.25O_2 \rightarrow NO + 1.5H_2O$	$r_1 = k_1 P_{NH_3}$	365.2 m^3 (kg s atm)$^{-1}$	73.6
$NH_3 + 0.75O_2 \rightarrow 0.5N_2 + 1.5H_2O$	$r_2 = k_2 P_{NH_3}$	8.5 m^3 (kg s atm)$^{-1}$	−28.4
$NO \rightarrow 0.5N_2 + 0.5O_2$	$r_3 = k_3 P_{NO}^2$	0.018 m^3 (kg s atm)$^{-1}$	3.76

$$R = k_{app}\left(\frac{P_{NH_3}^2}{P_{H_2}^3}\right)^{\beta} \quad (1)$$

$$k_{app} = k_{0pp}\exp\left(-\frac{E_{app}}{RT}\right) \quad (2)$$

Data stated in Section 2.1, Tables 1, 2 and Appendix A was used for the novel HAVAC process modelling.

Symbols and meaning

Symbols	Meaning
E_{app}	Activation energy
P_{NH_3}	Partial pressure of ammonia
P_{N_2}	Partial pressure of nitrogen
P_{H_2}	Partial pressure of hydrogen
LCOH	Levelized cost of hydrogen, $ per kg
TCR	Total capital requirement
FCF	Fixed charge cost factor
FOM	Fixed operating and maintenance cost per year,
VOC	Variable operating cost
M_{H_2}	Mass flowrate of produced hydrogen, kg h^{-1}
CF	Capacity factor
r	Discount rate
t	Plant design life, years
C_A	New scaled equipment cost
C_B	Base equipment cost
CI_A and CI_B	Annual chemical engineering plant index factors for reference year A and reference year B
S_A and S_B	New and base equipment capacity
X	Scaling factor

2.4 Economic evaluation

Economic evaluation of the novel HAVAC process was carried out in accordance with the methodology proposed by the Global CCS Institute[102] using key economic indicators such as the levelized cost of hydrogen (LCOH). The cost was calculated using eqn (3)–(6).[2,103,104] The fixed charge factor (FCF) converts the total capital requirement into uniform annual amounts at a discount rate over the lifetime of the plant. Total capital requirement (TCR), commonly referred to as CAPEX, is calculated using the installed cost for the main equipment and the assumptions stated in Tables 3 and 5. Balance of plant (BOP) costs include the cooling system, electricity, storage, make-up water, sanitary system, water discharge and solid wastes, *etc.* Bare equipment cost was obtained from various works as referenced in Table 3 and adjusted to year 2024 using eqn (6)[104] and the IHS global capital cost escalation index factor was applied. Similar to the Chemical Engineering plant index factor in Perry Hand book, IHS Markit, part of S&P Global, provide critical, reliable and up to date financial information including capital cost escalation index factor and database to

Table 3 Parameters and assumptions for economic analysis (CAPEX)

Economic model			
Equipment	HAVAC process	HAVAC process	Ref.
	Case 1 100% renewable electricity	Case 2 100% autothermal	
Description	BEC, $$1000	BEC, $$1000	—
Ammonia feed	1000 tonnes day^{-1}	1000 tonnes day^{-1}	—
HAVAC reactor, $1000	20 950	20 950	105
Gas heated cracker $1000	7452	7452	105
Air compressor package $1000	798	798	105
Dehydrator $1000	3467	3467	106
Nitrogen membrane $1000	20 514	20 514	107
PSA $1000	23 226	23 226	105
Separator $1000	1678	1678	106
Heat exchangers $1000	2818	2818	106

Table 4 Parameters and assumptions for economic analysis (OPEX)

Description	Values	Ref.
Operating labour	$60 000 per person-year	68
Operator per shift	16	105
Total shift per day	2	105
Maintenance, support, and administration	2.5% TOC	103
Property taxes and insurance	2% TOC	103

Table 5 Parameters and assumptions for economic analysis

Equipment	Number required	Bare equipment cost (BEC), $1000	Ref.
Capital cost escalation factor	1998:80 2007:170 2017:182 2020:205 2023:248		IHS Markit (downstream)
Capacity factor (CF)	0.95		
Plant design life	25 years		
Discount rate	12%		103
Engineering, procurement, and construction cost (EPCC)	8% of bare erected cost (BEC)		103
Process contingency	30% of BEC for MDEA unit, MEA unit, carbonator-reactor and membrane reactor; 0% for reference SMR plant		103
Project contingency	10% of (BEC + EPCC + process contingency)		103
Balance of project (BOP)	15% of (BEC + project contingency)		105
Total contingencies	Project contingency + process contingency		103
Total plant cost (TPC)	BEC + EPCC + total contingencies + BOP		103
Owner's cost	20.2% of TPC		103
Total overnight cost (TOC)	TPC + owner's cost		103
Total capital requirement (TCR)	1.14 × TOC		103

the industries both upstream and downstream. Their downstream data include refineries and petrochemicals which ammonia cracker plant falls under.

Assumptions used for the fixed operating and maintenance cost (FOM) and total capital cost (TCR) are summarised in Tables 3–5.

$$\mathrm{LCOH} = \frac{(\mathrm{TCR})(\mathrm{FCF}) + (\mathrm{FOM}) + (\mathrm{VOC})}{(M_{\mathrm{H_2}})(\mathrm{CF})(8760)} \quad (3)$$

$$\mathrm{VOC} = \text{Electricity cost} + \text{ammonia cost} \quad (4)$$

$$\mathrm{FCF} = \frac{r(1+r)^t}{(1+r)^t - 1} \quad (5)$$

$$C_{\mathrm{A}} = \left(\frac{\mathrm{CI_A}}{\mathrm{CI_B}}\right) C_{\mathrm{B}} \quad (6)$$

3. Results and discussions

3.1 Thermodynamic & kinetic evaluation of novel HAVAC process

3.1.1 Model validation and experimental comparisons. The model validation was undertaken drawing on experimental work by Cechetto *et al.* (2021)[100] and Di Carlos *et al.* (2014),[108] who utilized commercial catalysts: Alfa AesarTM (2% Ru) and Hypermec 10010TM (8% Ru), respectively. Kinetic constants from Richard *et al.* (2024),[109] detailed in Table 6, guided the fitting process under similar hydrodynamic conditions, employing an isothermal model. Simulations for validation were conducted across temperatures ranging from 400 °C to 500 °C and pressures of 4 bar and 10 bar, aligning closely with experimental setups. The reactor models demonstrated agreement with experimental data, typically within a 20% error margin, as illustrated in Fig. 2. At temperatures above 450 °C, model accuracy notably improved to less than 5%. Noteworthy observations at 500 °C revealed that ammonia conversion closely approached equilibrium levels in both experimental and modelled results. It is important to acknowledge that the validations were carried out using small-scale laboratory equipment. While this approach minimized potential influences from factors like gas feed impurities, mechanical erosion, and mass transfer limitations, which could affect catalyst activity in industrial-scale reactors, it may not fully capture the complexities of larger-scale industrial operations.

3.1.2 Thermodynamic equilibrium parametric analysis. Thermodynamic equilibrium parametric analysis was carried out for the novel HAVAC process shown in Fig. 1 in terms of ammonia conversion, hydrogen yield, hydrogen purity, hydrogen thermal efficiency and process thermal efficiency using eqn (7)–(9);[2] where '*n*' stands for relevant molar flowrates. Heating values for 100% ammonia gas (NH_3) and 100% hydrogen gas are simulated in Aspen Plus at standard conditions, and calculated as 22.5 MJ kg^{-1} and 142 MJ kg^{-1} respectively. Fig. 3 and 4 demonstrate that the optimized operating

Table 6 Main results for economic analysis

Equipment	100% renewable electricity mode	100% Air autothermal mode
Total bare equipment cost (BEC), $1000	80 903	80 903
Total EPCC, $1000	6472	6472
Total process contigency, $1000	0	0
Total project contigency, $1000	8737	8737
Balance of plant (BOP), $1000	13 446	13 446
Total plant cost (TPC), $1000	109 558	109 558
Owner's cost, $1000	22 131	22 131
Total overnight cost (TOC), $1000	131 688	131 688
Total capital requirement (TCR) or (CAPEX)	150 125	150 125
First year OPEX	233 800	212 416
Total hydrogen produced, kg h^{-1}	7398	5880
CAPEX cost of H_2 production	$0.31 per kg-$H_2$	$0.39 per kg-$H_2$
OPEX cost of H_2 production		
First year feedstock cost@$585 per tonnes of ammonia, first year electricity cost@$0.06 per kW h	$3.8 per kg-$H_2$	$4.34 per kg-$H_2$
First year LCOH	$4.1 per kg-$H_2$	$4.73 per kg-$H_2$

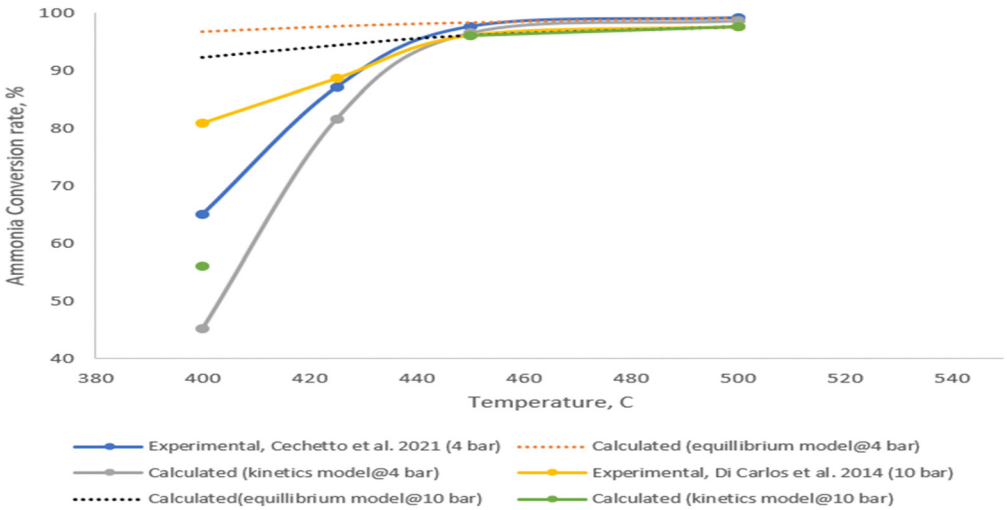

Fig. 2 Conversion *vs.* temperature for experimental data (Cechetto *et al.* (2021)[62] and Di Carlos *et al.* (2014)[73]), equilibrium model and kinetic model across temperatures ranging from 400 °C to 500 °C and pressures of 4 barg and 10 barg.

conditions for the HAVAC reactors are at a temperature of 700 °C and a pressure of 8 barg. Under these conditions, the overall ammonia conversion was calculated to be a minimum of 99.6% for both 100% air autothermal and 100% renewable electricity operations. The hydrogen yield ranged from 84% to 99.5%, contingent upon the operational mode. The lower hydrogen yield of 84% observed under 100% air autothermal mode can be attributed to the fact that a portion of the hydrogen produced is consumed as fuel to provide the necessary energy for the endothermic decomposition of ammonia. Fig. 5 and 6 present the calculated process thermal efficiency across a range of reactor temperatures (400 °C to 1000 °C) and pressures (2 barg to 20 barg) for both operational modes. The optimal process thermal efficiency was found to be between 94% and 94.5% at the ideal pressure of 800 kPa and temperature of 700 °C. This efficiency range reflects the high performance of the HAVAC process in converting ammonia and producing hydrogen while maintaining significant thermal efficiency.

The detailed validation and parametric analysis confirm the HAVAC process's robustness and efficiency. The alignment of model predictions with experimental data across a range of conditions demonstrates the reliability of the model, particularly at elevated temperatures where accuracy improved. The comprehensive thermodynamic analysis underscores the process's potential, with optimal conditions identified for maximum efficiency and yield. The small-scale experimental validations provide a strong foundation, though it is essential to consider the implications of scaling up. The transition from laboratory to industrial scale may introduce additional complexities that could affect catalyst performance and overall process efficiency. Future work should focus on bridging this gap by conducting pilot-scale experiments and refining models to account for industrial-scale variables.

Overall, the HAVAC process exhibits significant promise, with high ammonia conversion rates and favorable thermal

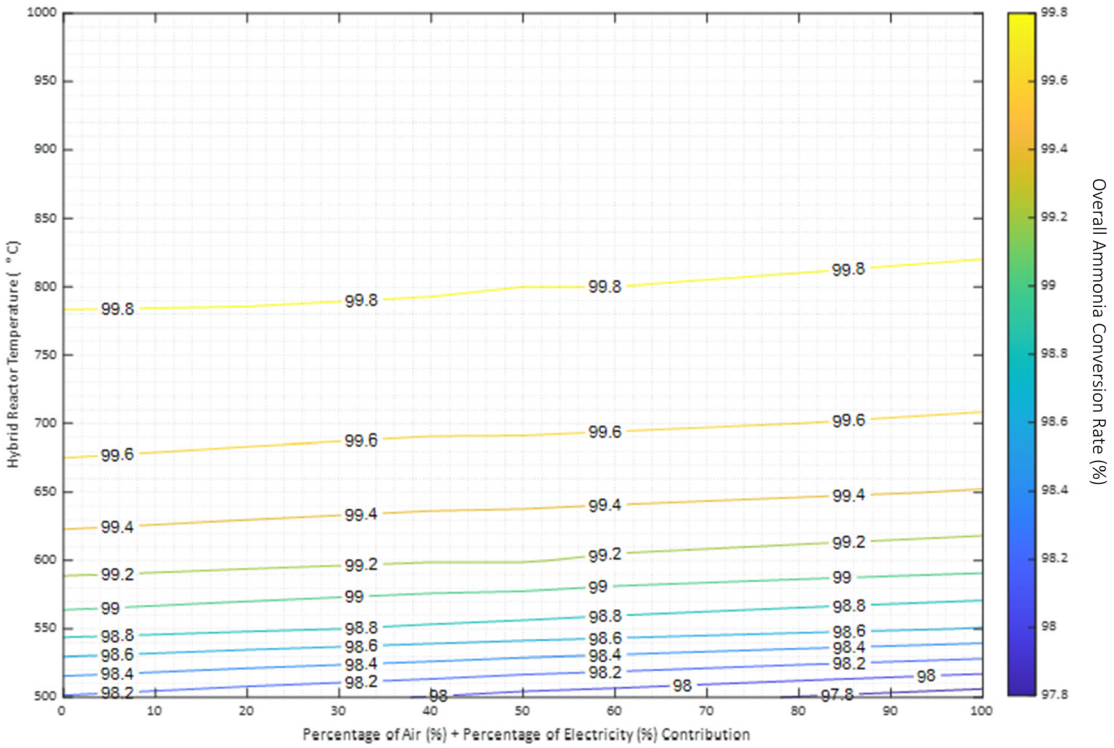

Fig. 3 Overall ammonia conversion at different air-autothermal and renewable electricity overall thermal contribution expressed as percentage. Reactor pressure at 8 barg.

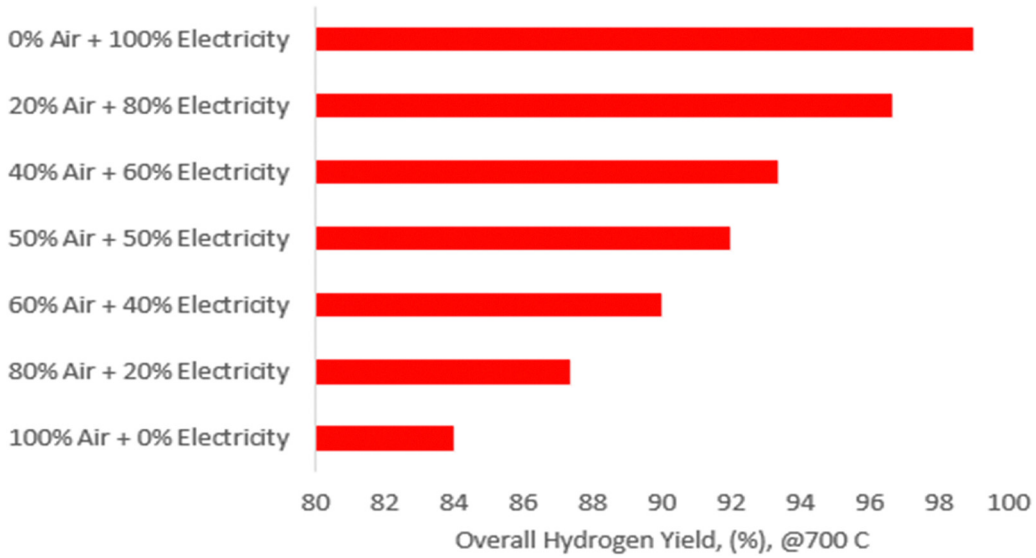

Fig. 4 Overall hydrogen yield (%) at different air-autothermal and renewable electricity overall thermal contribution expressed as percentage and reactor pressure at 8 barg.

efficiencies, making it a compelling option for advancing hydrogen production technologies.

3.2 HAVAC process reactor performance

3.2.1 Gas heated cracker (GHC). The gas heated cracker (GHC) reactor is designed to enhance the efficiency of the main HAVAC reactor (hybrid air-volt ammonia cracker) by significantly reducing its overall heat demand. This is achieved by leveraging the hot product gas from the HAVAC reactor as a heating medium to provide the necessary endothermic heat for the initial cracking of the ammonia feed. The GHC reactor is engineered as a monolithic metallic shell with a multi-tubular,

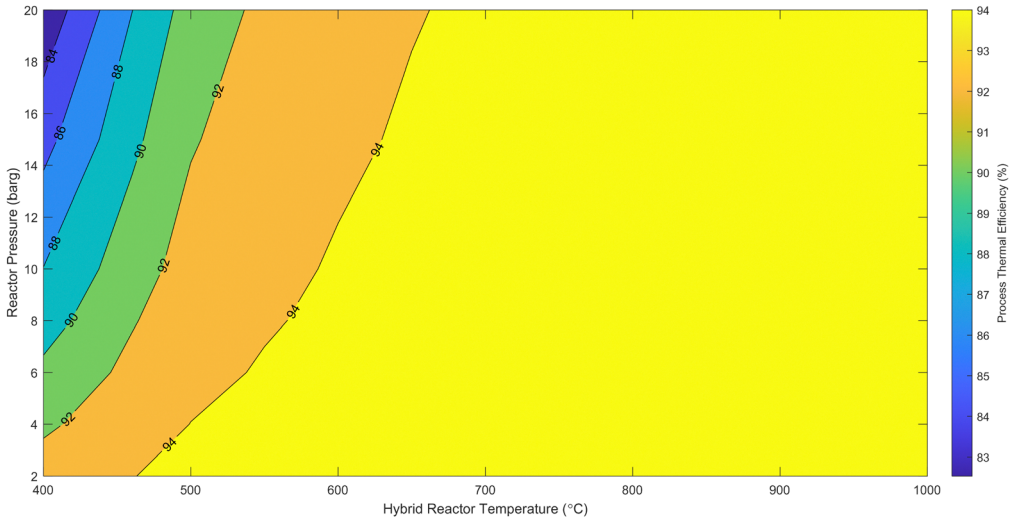

Fig. 5 Novel process thermal efficiency at different hybrid cracker pressure and temperature for 100% renewable electricity operation.

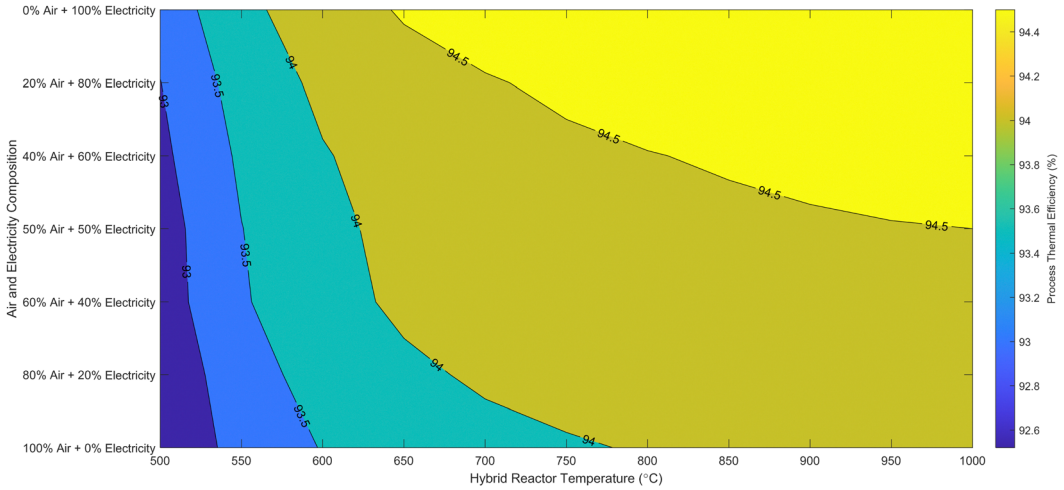

Fig. 6 Novel process thermal efficiency at different hybrid cracker temperature and air-autothermal and renewable electricity overall thermal contribution expressed as percentage. Reactor pressure at 800 kPa.

multi-pass configuration. This design maximizes heat transfer efficiency and is packed with a ruthenium catalyst to facilitate the cracking reaction. The operational design involves the counter-current flow of gases: the hot product gas from the HAVAC reactor enters the GHC reactor from the top, while the ammonia feed gas is introduced from the bottom, as depicted in Fig. 1. Fig. 7(a) and (b) present a comparative analysis of the kinetic and thermodynamic performance of the GHC reactor under two distinct operational modes: 100% renewable electricity and 100% air autothermal operation. For a feed gas flow rate of 2446 kmol h^{-1} (equivalent to 1000 tonnes day^{-1} of ammonia), the thermodynamic equilibrium ammonia conversion achieved during operation with 100% renewable electricity is 25.9%. This results in a total product gas flow of 3081 kmol h^{-1} from the GHC reactor. In contrast, during 100% air autothermal operation, the ammonia conversion reaches 45.9%, and the total product gas flow from the GHC increases to 3568.6 kmol h^{-1}. The kinetic model, which accounts for dynamic reaction rates and non-ideal behaviors, predicts ammonia conversions of 25.8% under renewable electricity operation and 31% under air autothermal operation. These kinetic values align reasonably well with the thermodynamic equilibrium predictions, indicating that the model accurately represents the reactor's performance under different operating conditions. The observed increase in ammonia conversion within the GHC during air autothermal operation compared to renewable electricity operation can be attributed to the higher sensible heat within the GHC reactor. This increase is due to the greater volume of hot product gas from the HAVAC reactor,

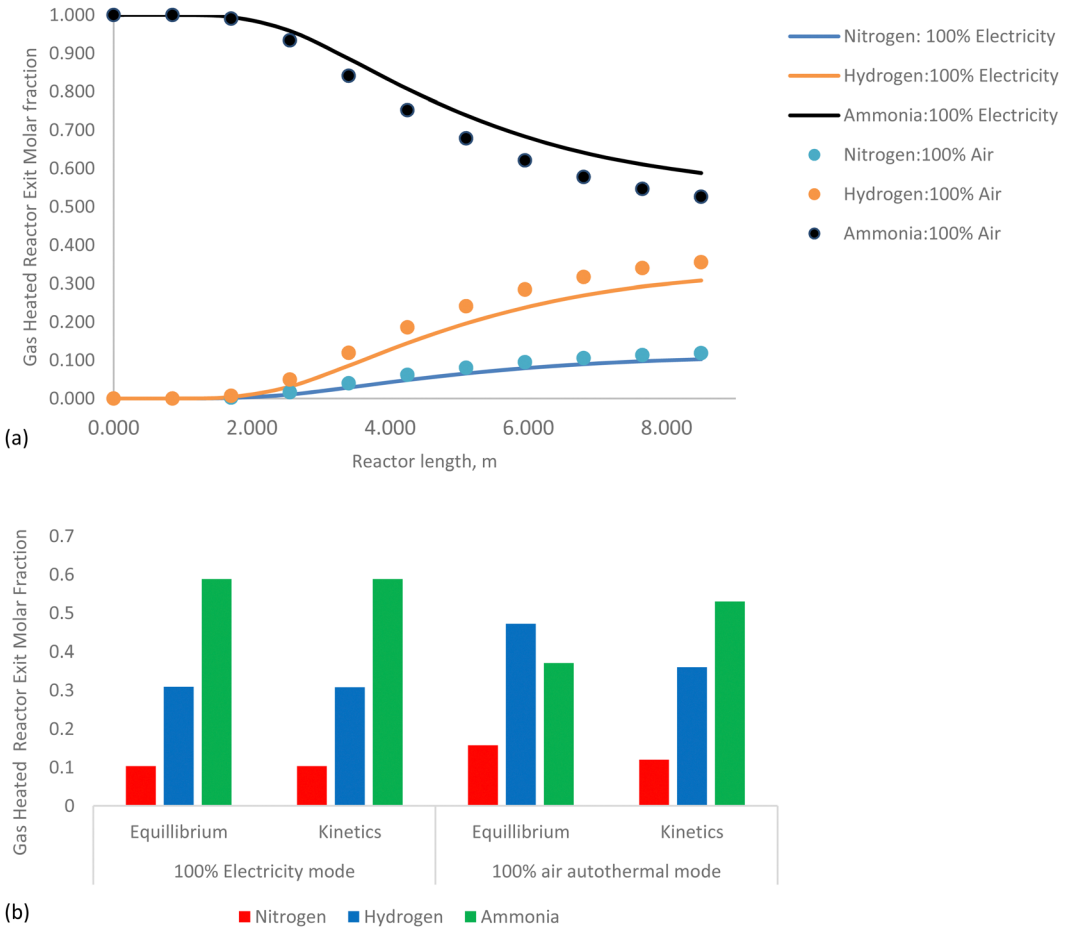

Fig. 7 (a) Kinetic model for gas heated cracker reactor performance for both 100% renewable electricity and 100% air autothermal mode operation at reactor pressure of 8 barg and 700 °C, (b) equilibrium and kinetic model for gas heated cracker reactor performance for both 100% renewable electricity and 100% air autothermal mode operation 8 barg.

which, during air autothermal operation, contains steam as one of the products gas. This enhances the heating capacity of the product gas, thereby improving the overall heat transfer and increasing the efficiency of ammonia cracking in the GHC reactor.

In summary, the gas heated cracker reactor effectively utilizes the heat from the HAVAC reactor, optimizing overall energy consumption and improving ammonia conversion rates.

3.2.2 Hybrid air-volt ammonia cracker. The hybrid air-volt ammonia cracker (HAVAC) reactor is a pivotal component in

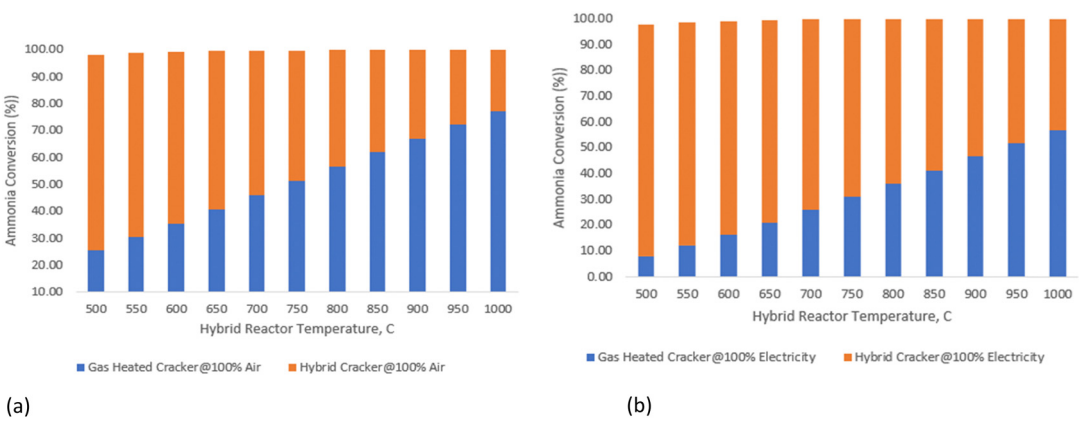

Fig. 8 (a) Ammonia conversion (%) contribution between gas heated cracker reactor and HAVAC reactor for 100% air-autothermal operation at 8 barg. (b) Ammonia conversion (%) contribution for gas heated cracker and HAVAC Reactor for 100% renewable electricity operation at 8 barg.

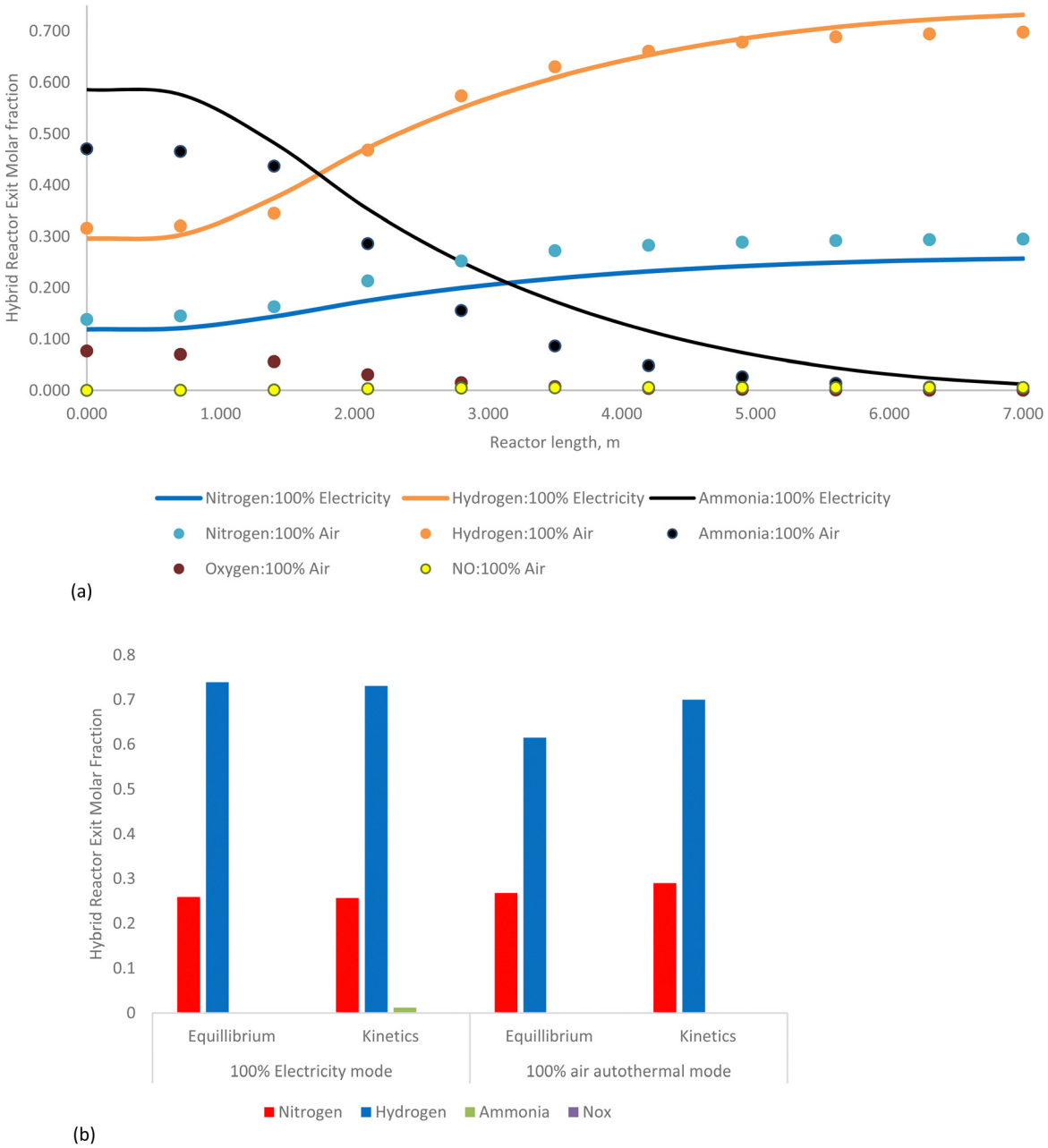

Fig. 9 (a) Kinetic model for hybrid air-volt ammonia cracker (HAVAC) reactor performance for both 100% renewable electricity and 100% air autothermal mode operation at reactor pressure of 8 barg and temperature of 700 °C. (b) Equilibrium and kinetic model for hybrid air-volt ammonia cracker (HAVAC) reactor for both 100% renewable electricity and 100% air autothermal mode operation at reactor pressure of 8 barg and temperature of 700 °C.

the process. It plays a dual role: achieving near-complete ammonia conversion while also supplying the necessary thermal energy for the upstream gas heated cracker (GHC). As illustrated in Fig. 3, the HAVAC reactor excels in driving ammonia conversion rates to nearly 99.4%, thereby underscoring its critical function in the overall system. The operational flexibility of the HAVAC reactor is facilitated by its ability to utilize heat from two distinct sources: renewable electricity *via* electromagnetic inductive heating and autothermal reactions using ammonia fuel combined with air. This flexibility allows the HAVAC reactor to be integrated with the product gas from the GHC, which is either combined with lean air (air from which most nitrogen has been removed using a nitrogen membrane system) or directly fed into the HAVAC reactor. Fig. 8(a) and (b) show the contributions in terms of overall ammonia conversion between the GHC reactor and HAVAC reactor at different reactor temperatures and pressure of 800 kPa. For 100% air-autothermal operation, the

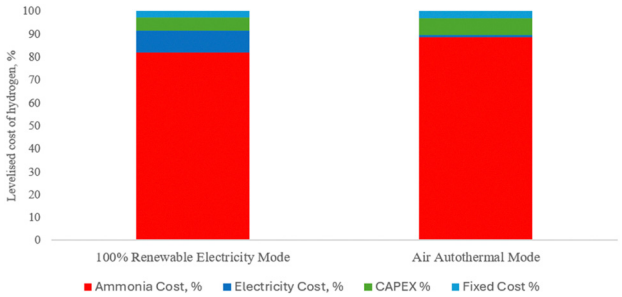

Fig. 10 Distribution of different components of the levelized cost.

calculated thermodynamic equilibrium ammonia conversion contributions (Fig. 8a) for GHC reactor and HAVAC reactor is 46% and 54% respectively. Similarly, for 100% renewable electricity mode as per Fig. 8(b) the calculated thermodynamic equilibrium ammonia conversion contributions for GHC reactor and HAVAC reactor is 26% and 74% respectively. Fig. 9(a) and (b) provide a comparative analysis of the HAVAC reactor's performance under two operational modes: 100% renewable electricity and 100% air autothermal operation. For a feed gas flow rate of 3155 kmol h^{-1}, which includes 74.6 kmol h^{-1} of unreacted recycled ammonia, the thermodynamic equilibrium ammonia conversion achieved with 100% renewable electricity is 99.4%. This high conversion rate results in a total product gas flow of 4968 kmol h^{-1} from the HAVAC reactor. During 100% air autothermal operation, the ammonia conversion similarly reaches 99.4%, but the total product gas flow increases to 5023 kmol h^{-1}, with 11.6% of this being steam.

The kinetic model, which accounts for dynamic reaction rates and non-ideal behaviors, shows ammonia conversions of 96.8% under renewable electricity operation and 96.5% under air autothermal operation. These kinetic values are in close agreement with the thermodynamic equilibrium predictions, confirming the model's reliability in representing the reactor's performance under varying operational conditions.

In summary, the HAVAC reactor not only achieves near-complete ammonia conversion but also efficiently integrates with the GHC process to optimize overall system performance. Its dual heating capability—renewable electricity and autothermal reaction—offers operational flexibility and efficiency.

$$\text{Ammonia conversion} = \frac{n_{NH_{3(IN)}} - n_{NH_{3(OUT)}}}{n_{NH_{3(IN)}}} \times 100\% \quad (7)$$

$$\text{Hydrogen yield } (\%) = \frac{\text{Actual hydrogen produced}}{\text{Theoretical hydrogen produced}} \times 100\% \quad (8)$$

$$\text{Process thermal efficiency } (\%) = \frac{\text{Molar flow of } H_{2(OUT)} \times HHV_{H_2}}{\text{Molar flow of } NH_{3(FEED)} \times HHV_{NH_3} + \text{Net heating duty}} \times 100\% \quad (9)$$

3.3 Economic analysis

An in-depth economic evaluation of the novel hybrid air-volt ammonia cracker (HAVAC) process was conducted using methodologies established by the Global CCS Institute.[67] This assessment utilized key economic indicators, particularly the levelized cost of hydrogen (LCOH), to determine the financial viability of the process. The foundational approach for this economic analysis is detailed in Section 2.4.

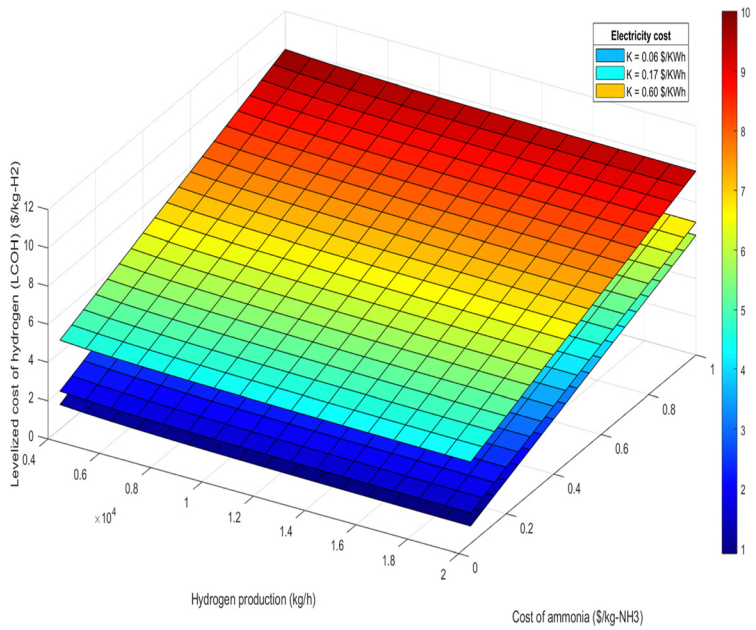

Fig. 11 LCOH at different hydrogen production and different ammonia cost for 100% renewable electricity mode.

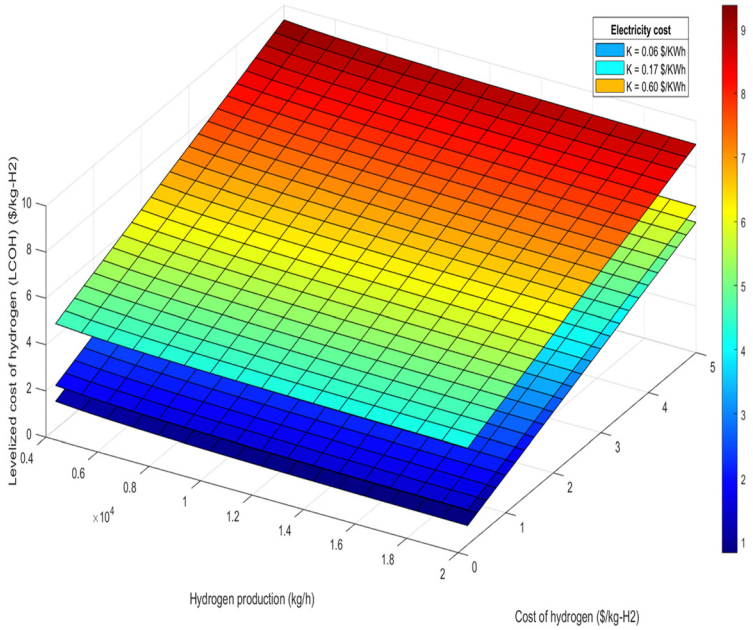

Fig. 12 LCOH at different hydrogen production and different hydrogen cost for 100% renewable electricity mode.

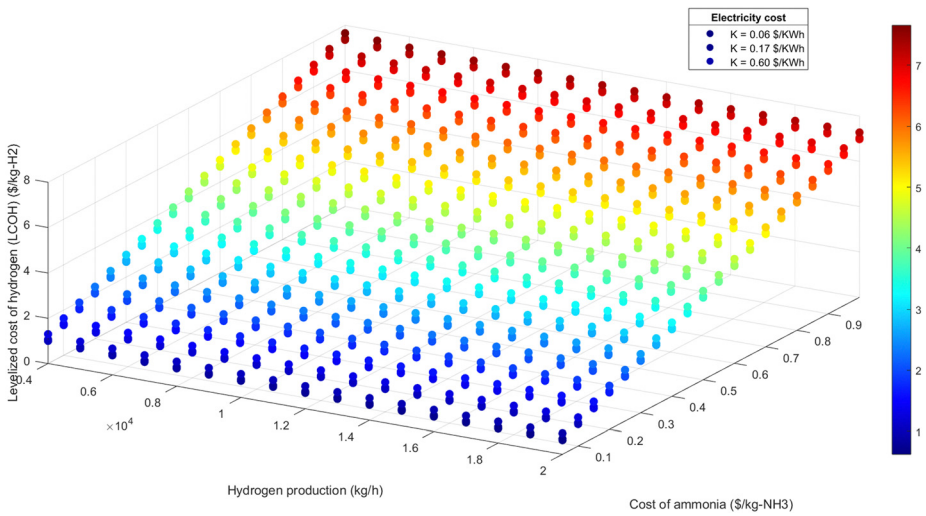

Fig. 13 LCOH at different hydrogen production and different ammonia cost for 100% air-autothermal mode.

3.3.1 Economic performance overview. Table 6 and Fig. 10–18 present the results from the comprehensive economic parametric analysis of the HAVAC process. The analysis specifically evaluates a plant processing an ammonia feed of 1000 tonnes per day (equivalent to 41 667 kg h^{-1}), producing between 5880 kg h^{-1} and 7390 kg h^{-1} of hydrogen, depending on the operational mode: 100% renewable electricity or 100% air-autothermal. The LCOH for the HAVAC process is calculated to range from \$4.10 per kg-H_2 to \$4.73 per kg-H_2. This variation is influenced by the mode of operation and associated costs. Fig. 10 illustrates the cost distribution, revealing that ammonia feedstock comprises the majority of the total cost, accounting for 82% to 88%. Electricity costs constitute nearly 10% of the total expenditure in the 100% renewable electricity mode, reflecting its role as the primary energy source for heating in the HAVAC reactor. In contrast, during the 100% air autothermal operation, electricity costs drop to approximately 1%, as it primarily supports air compressors and other utilities.

3.3.2 Parametric sensitivity analysis. Fig. 11–16 provide insights into how variations in key parameters affect the LCOH. These parameters include hydrogen production rates, ammonia feed rates, and the costs of ammonia and renewable electricity.

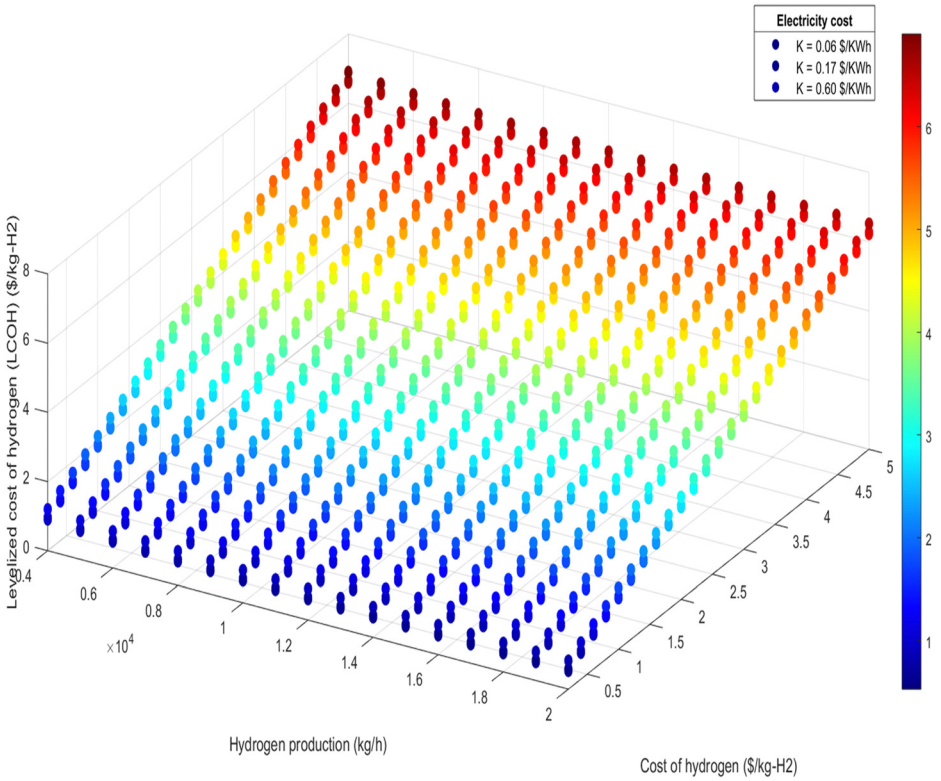

Fig. 14 LCOH at different hydrogen production and different hydrogen cost for 100% air-autothermal mode.

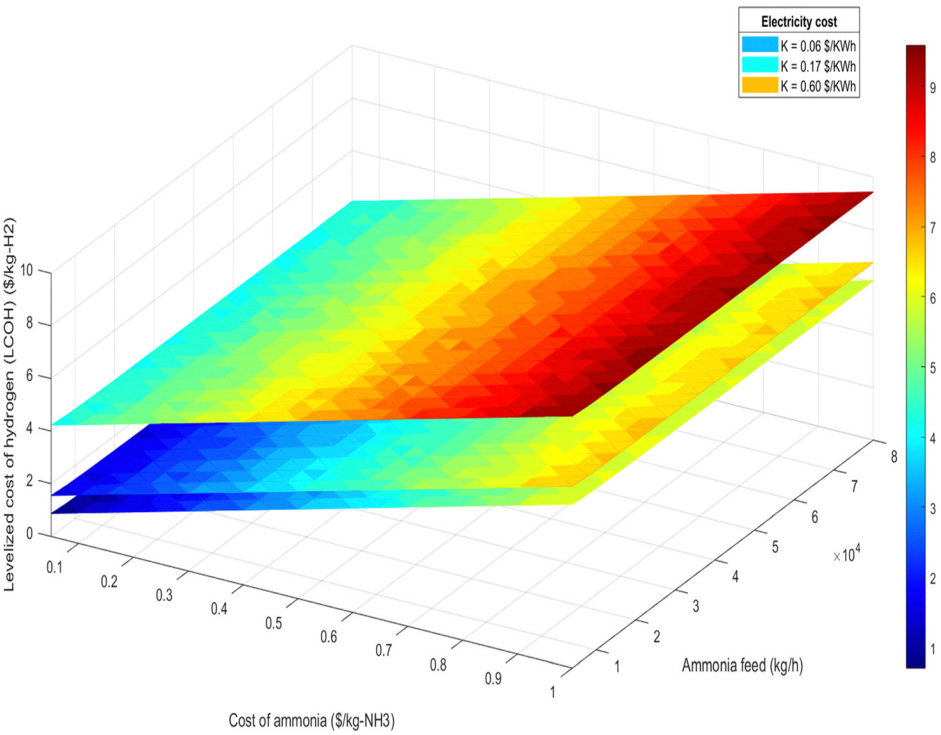

Fig. 15 LCOH at different ammonia production and different ammonia cost for 100% renewable electricity mode.

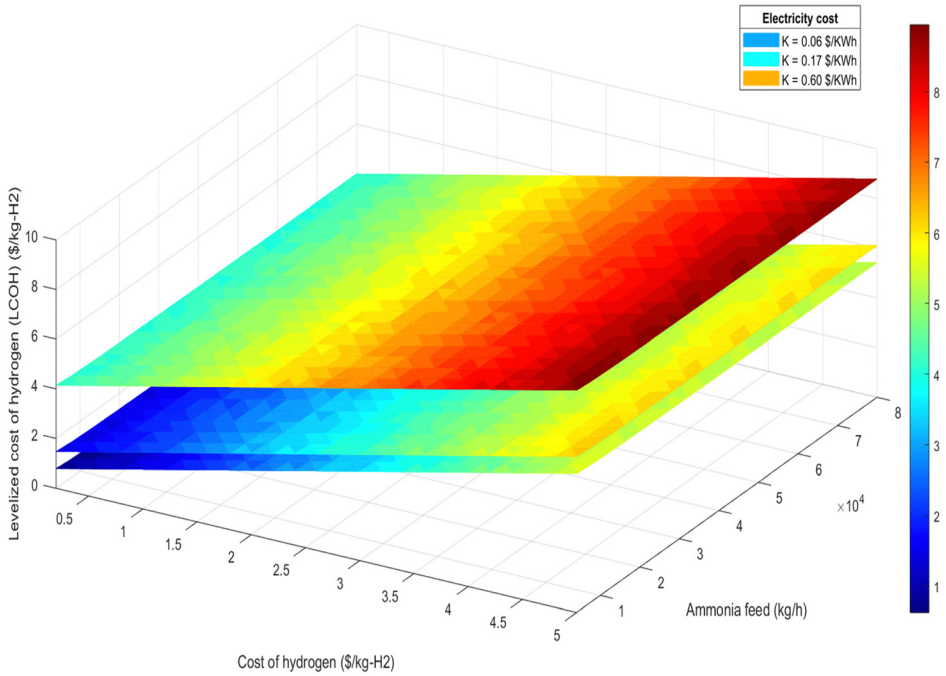

Fig. 16 LCOH at different ammonia production and different hydrogen cost for 100% renewable electricity mode.

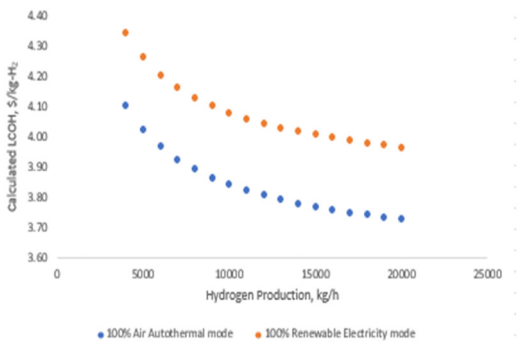

Fig. 17 LCOH at different hydrogen production (ammonia cost used: \$0.550 per kg-NH_3).

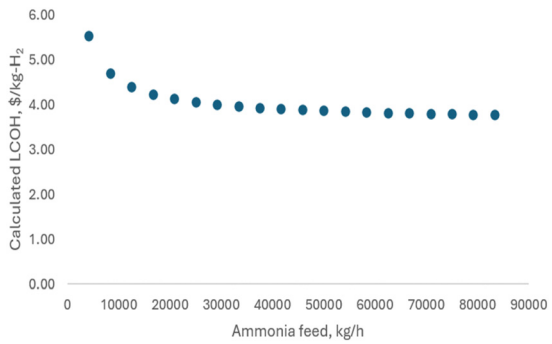

Fig. 18 LCOH at different ammonia feed (ammonia cost used: \$0.550 per kg-NH_3).

• Electricity cost sensitivity: the impact of electricity costs on LCOH was analyzed across three sensitivity scenarios: \$0.06 per kW h, \$0.17 per kW h, and \$0.60 per kW h. During 100% renewable electricity operation, electricity costs can affect LCOH by up to 10%, as shown in Fig. 11 and 12. In this scenario, higher electricity prices lead to a proportionate increase in LCOH. Conversely, during 100% air-autothermal operation (Fig. 13 and 14), the impact of electricity cost changes is minimal due to the reduced electricity demand.

• Ammonia and hydrogen costs: the analysis indicates that increases in ammonia or hydrogen costs lead to higher LCOH. However, the relative increase in LCOH diminishes as these costs rise, suggesting a decreasing sensitivity of LCOH to higher feedstock or product costs (Fig. 11–14).

• Ammonia feed rate and hydrogen production: the LCOH decreases with increased ammonia feed rates or higher hydrogen production levels. This is attributed to economies of scale and the more efficient utilization of resources, as demonstrated in Fig. 15 and 16.

3.3.3 Comparative analysis and economic advantage. Fig. 17 summarizes the comparative economic performance of the two operational modes. It indicates that the 100% renewable electricity mode generally exhibits a lower LCOH compared to the 100% air-autothermal mode, highlighting a potential economic advantage for using renewable electricity. This outcome is particularly relevant in the context of reducing operational costs and enhancing the economic feasibility of the HAVAC process.

Fig. 18 further explores the relationship between LCOH and ammonia feed rate, illustrating that larger plant sizes result in reduced hydrogen production costs. This trend underscores the economic benefit of scaling up the plant to achieve lower LCOH.

4. Conclusions

This paper introduces the hybrid air-volt ammonia cracker (HAVAC), a novel advancement in the field of hydrogen production from ammonia, specifically designed to address several gaps identified in existing ammonia cracking technologies.

1. Addressing process efficiency and flexibility: the HAVAC process presents a centralized solution capable of efficiently converting blue or green ammonia into high-purity hydrogen for fuel cell applications. It achieves an impressive thermal efficiency of 94% to 95%, surpassing current state-of-the-art technologies. This efficiency is bolstered by HAVAC's ability to operate with renewable electricity ranging from 0% to 100%, thus providing flexibility in response to varying energy availability and costs. Additionally, HAVAC can function in autothermal mode using air, further enhancing its operational versatility.

2. Ensuring fuel cell-grade hydrogen production: the HAVAC process integrates advanced purification technologies to produce high-purity hydrogen suitable for fuel cells. This capability overcomes the limitations observed in current systems, where high-purity hydrogen production is often constrained.

3. Reducing operational costs: economic feasibility is a common issue with ammonia cracking technologies due to high operational costs and complex reactor designs. The HAVAC process addresses these concerns by employing cost-effective materials and innovative reactor designs, which significantly reduce operational and maintenance expenses. This approach aims to lower the overall levelized cost of hydrogen (LCOH), with costs ranging from $3.8 per kg-H2 to $6 per kg-H2 depending on ammonia prices and plant capacity.

4. Facilitating scaling up production: scaling ammonia cracking technology to meet industrial demands remains a challenge. The HAVAC is designed with scalability in mind, featuring modular components that facilitate the transition from pilot-scale to commercial-scale operations. This design supports large-scale hydrogen production and addresses the need for efficient, large-scale operations.

5. Addressing environmental and economic concerns: in alignment with global initiatives to reduce greenhouse gas emissions, such as those outlined in the COP28 agreement, the HAVAC process utilizes ammonia as a hydrogen carrier to mitigate storage and transportation challenges. The centralized nature of the HAVAC process allows for efficient large-scale hydrogen production, making it a viable solution for widespread distribution. The process also incorporates renewable electricity, minimizing greenhouse gas emissions compared to traditional fossil fuel-based systems. However, it does produce nitrogen oxides (NOx) as a byproduct during autothermal operation, necessitating effective waste management strategies, such as integrating molecular sieve beds for NOx removal.

Future research directions: future research should focus on scaling up from laboratory to pilot and industrial scales, addressing complexities such as catalyst performance variability, mechanical wear, and operational stability. Enhancing process control systems, improving catalyst longevity, and developing robust scaling-up methodologies will be crucial. Additionally, further research into reducing operational costs, optimizing waste management techniques, and exploring alternative catalysts will be vital for ensuring the commercial viability of the HAVAC process.

Conclusion: the HAVAC process stands out as a promising and sustainable technology for hydrogen production. Its combination of high efficiency, operational flexibility, and economic viability positions it as a frontrunner in the transition toward a low-carbon hydrogen economy. By addressing key challenges in ammonia cracking, the HAVAC process contributes significantly to the realization of a carbon-free hydrogen future.

Data availability

This is a statement to confirm that all data used for the ''Novel Carbon-Free Innovation in Centralised Ammonia Cracking For A Sustainable Hydrogen Economy: The Hybrid Air-Volt Ammonia Cracker (HAVAC) Process'' are accurate and can be made available upon request.

Conflicts of interest

There are no conflicts to declare.

Appendix

Appendix A

Tables 7 and 8.

Table 7 Kinetic law parameters fitted using the Temkin–Pyzhev

	k_0 [kmol m^{-3} h^{-1} bar$^{-\beta}$]	E_0 [kJ mol^{-1}]	β [—]
Cechetto *et al.* (2021)[100]	4.09×10^{14}	187 683	0.560
Di Carlo *et al.* (2014)[108]	4.09×10^{12}	149 628	0.799

Table 8 Process control system for novel HAVAC process

Control parameter	Description of control
Feed flowrate	Feed flow rate to process is maintained by FIC-003.
Air pressure	Air pressure is maintained by PIC-001 by switching on/off the number of air compressors online. Typical screw compressors are used.
Hybrid air cracker temperature	• The hybrid air-volt cracker reactor outlet temperature is controlled by duty TIC-001A and assist TIC-001B. • Duty TIC-001A is set at 600 °C/700 °C to maintain reactor outlet temperature by modulating renewable electricity voltage through the voltage regulator (VR-001), during periods of renewable electricity availability. • As renewable electricity power declines during the night or during periods of low/no availability, reactor temperature drops and this activates the assist controller, TIC-001B, set at 10 °C lower than TIC-001A. • The assist controller, TIC-001B is cascaded with the air flow controller, FIC-001 which determines the amount of air required to achieve the required reactor temperature.
Air flowrate	The air flow transmitter, FIT-001 feeds the required air into a feed forward ratio controller, FFC-001.
Ammonia fuel flowrate	Feed forward ratio controller, FFC-001 determine the amount of ammonia fuel required through a stoichiometric ratio and feeds this to FIC-002 which controls the amount of ammonia fuel.
Heat	The combustion of ammonia and air releases the required heat required for the endothermic ammonia decomposition reaction.

Notes and references

1 Release UCP, UN Climate Press Release, dated 13 December 2023, (https://www.unfcc.int/news/COP28-agreement-signals-beginning-of-end-of-the-fossil-fuel-era) 13th December, 2023 13 December 2023.
2 C. Eluwah, P. S. Fennell, C. J. Tighe, A. A. A. Dawood, C. Eluwah, P. S. Fennell, C. J. Tighe and A. A. Dawood, A novel technological blue hydrogen production process: industrial sorption enhanced autothermal membrane (ISEAM), *Energy Adv.*, 2023, **2**(9), 1476–1494.
3 H. Lee, B. Lee, M. Byun and H. Lim, Comparative techno-economic analysis for steam methane reforming in a sorption-enhanced membrane reactor: simultaneous H_2 production and CO_2 capture, *Chem. Eng. Res. Des.*, 2021, **171**, 383–394.
4 S. Surya Pratap, Z. G. Solanki, S. Marino, R. J. Davis, W. S. Epling and L. C. Grabow, Methane partial oxidation under periodic reaction conditions on Pt/Al_2O_3, *React. Chem. Eng.*, 2024, **9**, 1489.
5 B. Christian Enger, R. Lødeng and A. Holmen, *Appl. Catal., A*, 2008, **346**, 1–27.
6 A. T. Ashcroft, A. K. Cheetham, M. L. H. Green and P. D. F. Vernon, *Nature*, 1991, **352**(6332), 225–226.
7 M. A. Nemitallah, A. A. Alnazha, U. Ahmed, M. El-Adawy and M. A. Habib, Review on techno-economics of hydrogen production using current and emerging processes: status and perspectives, *Results Eng.*, 2024, **21**, 101890.
8 K. Aasberg-Petersen, T. S. Christensen, C. S. Nielsen and I. Dybkjær, Recent developments in autothermal reforming and pre-reforming for synthesis gas production in GTL applications, *Fuel Process. Technol.*, 2003, **83**(1–3), 253–261.
9 J. D. Holladay, J. Hu, D. L. King and Y. Wang, An overview of hydrogen production technologies, *Catal. Today*, 2009, **139**(4), 244–260.
10 F. Qureshi, M. Yusuf, A. Khan, H. Ibrahim, B. Chukwuemeka Ekeoma, H. Kamyab, M. M. Rahman, A. Kumar Nadda and S. Chelliapan, A State-of-The-Art Review on the Latest trends in Hydrogen production, storage, and transportation techniques, *Fuel*, 2023, **340**, 127574.
11 T. Paulmier and L. Fulcheri, Use of non-thermal plasma for hydrocarbon reforming, *Chem. Eng. J.*, 2005, **106**, 59–71, DOI: 10.1016/J.CEJ.2004.09.005.
12 L. C. D. Bromberg, A. Rabinovich and N. Alexeev, Plasma catalytic reforming of methane, *Int. J. Hydrogen Energy*, 1998, **24**, 1131–1137, DOI: 10.2172/305623.
13 Th Hammer, Th Kappes and M. Baldauf, Plasma catalytic hybrid processes: gas discharge initiation and plasma activation of catalytic processes, *Catal. Today*, 2004, **89**, 5–14, DOI: 10.1016/J.CATTOD.2003.11.001.
14 S. A. Grigoriev, V. N. Fateev, D. G. Bessarabov and P. Millet, Current status, research trends, and challenges in water electrolysis science and technology, *Int. J. Hydrogen Energy*, 2020, **45**, 26036–26058.
15 E. Zhang and W. Song, Review—Self-Supporting Electrocatalysts for HER in Alkaline Water Electrolysis, *Electrochem. Soc.*, 2024, **171**, 052503.
16 V. Madadi Avargani, S. Zendehboudi, N. M. Cata Saady and M. B. Dusseault, A comprehensive review on hydrogen production and utilization in North America: prospects and challenges, *Energy Convers. Manage.*, 2022, **269**, 115927.
17 R. Y. Kannah, S. Kavitha, O. P. Karthikeyan, G. Kumar, N. V. Dai-Viet and J. R. Banu, Techno-economic assessment of various hydrogen production methods–A review, *Bioresour. Technol.*, 2021, **319**, 124175.
18 M. Ni, D. Y. C. Leung, M. K. Leung and K. Sumathy, An overview of hydrogen production from biomass, *Fuel Process. Technol.*, 2006, **87**(5), 461–472.
19 S. A. Arni, Comparison of slow and fast pyrolysis for converting biomass into fuel, *Renewable Energy*, 2018, **124**, 197–201.

20 S. E. Lindquist and C. Fell, Fuels – Hydrogen Production Photoelectrolysis, *Encycl. Electrochem. Power Sources*, 2009, 369–383, DOI: 10.1016/B978-044452745-5.00319-1.
21 C.-H. Chen, C.-T. Yu and W.-H. Chen, Improvement of steam methane reforming via in-situ CO_2 sorption over a nickel-calcium composite catalyst, *Int. J. Hydrogen Energy*, 2021, **46**(31), 16655–16666.
22 J. R. Fernández and J. Carlos Abanades, Sorption enhanced reforming of methane combined with an iron oxide chemical loop for the production of hydrogen with CO_2 capture: conceptual design and operation strategy, *Appl. Therm. Eng.*, 2017, **125**, 811–822.
23 F. H. Alshafei, L. T. Minard, D. Rosales, G. Chen and A. Simonetti Dante, Improved Sorption-Enhanced Steam MethaneReforming via Calcium Oxide–Based Sorbents with Targeted Morphology, *Energy Technol.*, 2019, **7**(3), 1800807.
24 H. Yu, H. Sun, G. Bao, H. Liu, J. Hu and H. Wang, Computational fluid dynamics study of hydrogen production by sorption enhanced steam ethanol reforming process in fluidized bed, *Fuel*, 2023, **344**, 128043.
25 B. Lee and H. Lim., Cost-competitive methane steam reform ing in a membrane reactor for H_2 production: technical and economic evaluation with a window of a H_2 selectivity, *Int. J. Energy Res.*, 2019, **43**(4), 1468–1478.
26 M. A. Murmura, S. Cerbelli and M. C. Annesini., An equilibrium theory for catalytic steam reforming in membrane reactors, *Chem. Eng. Sci.*, 2017, **160**, 291–303.
27 H. Lee, A. Kim, B. Lee and H. Lim, Comparative numerical analysis for an efficient hydrogen production via a steam methane reforming with a packed-bed reactor, a membrane reactor, and a sorption-enhanced membrane reactor, *Energy Convers. Manage.*, 2020, **213**, 112839.
28 K. Ghasemzadeh, R. Zeynali, A. Basile and A. Iulianelli, CFD analysis of a hybrid sorption-enhanced membrane reactor for hydrogen production during WGS reaction, *Int. J. Hydrogen Energy*, 2017, **42**(43), 26914–26923.
29 S. A. Wassie, A. Zaabout, F. Gallucci, S. Cloete, M. van Sint Annaland and S. Amini, Hydrogen production with integrated CO_2 capture in a novel gas switching reforming reactor: proof-of-concept, *Int. J. Hydrogen Energy*, 2017, **42**, 14367e14379.
30 L. G. Velazquez-Vargas, *Development of Chemical Looping Gasification Processes for the Production of Hydrogen from Coal*, The Ohio State University, 2007.
31 P. Chiesa, G. Lozza, A. Malandrino, M. Romano and V. Piccolo, Three-reactors chemical looping process for hydrogen production, *Int. J. Hydrogen Energy*, 2008, **33**(9), 2233–2245.
32 H. Bahzad, N. Shah, N. M. Dowell, M. Boot-Handford, S. M. Soltani and M. Ho, *et al.*, Development and techno economic analyses of a novel hydrogen production process via chemical looping, *Int. J. Hydrogen Energy*, 2019, **44**(39), 21251–21263.
33 A. Hajizadeh, M. Mohamadi-Baghmolaei, N. M. Cata Saady and S. Zendehboudi., Hydrogen production from biomass through integration of anaerobic digestion and biogas dry reforming, *Appl. Energy*, 2022, **309**, 118442.
34 U. Shreenag Meda, N. Bhat, A. Pandey, K. N. Subramanya and M. A. Lourdu Antony Raj, Challenges associated with hydrogen storage systems due to the hydrogen embrittlement of high strength steels, *Int. J. Hydrogen Energy*, 2023, **48**(47), 17894–17913.
35 R. Moradi and K. M. Groth, Hydrogen storage and delivery: review of the state of the art technologies and risk and reliability analysis, *Int. J. Hydrogen Energy*, 2019, **44**(23), 12254–12269.
36 A. M. Elberry, J. Thakur, A. Santasalo-Aarnio and M. Larmi, Large-scale compressed hydrogen storage as part of renewable electricity storage systems, *Int. J. Hydrogen Energy*, 2021, **46**(29), 15671–15690.
37 A. Trautmann, G. Mori, M. Oberndorfer, S. Bauer, C. Holzer and C. Dittmann, Hydrogen Uptake and Embrittlement of Carbon Steels in Various Environments, *Materials*, 2020, **13**(16), 3604.
38 S. Singh, S. Jain, P. S. Venkateswaran, A. K. Tiwari, M. R. Nouni and J. K. Pandey, *et al.*, Hydrogen: a sustainable fuel for future of the transport sector, *Renewable Sustainable Energy Rev.*, 2015, **51**, 623–633.
39 A. M. Abdalla, S. Hossain, O. B. Nisfindy, A. T. Azad, M. Dawood and A. K. Azad, Hydrogen production, storage, transportation and key challenges with applications: a review, *Energy Convers. Manage.*, 2018, **165**, 602–627.
40 F. Ustolin, N. Paltrinieri and F. Berto, Loss of integrity of hydrogen technologies: a critical review, *Int. J. Hydrogen Energy*, 2020, **45**(43), 23809–23840.
41 C. Makhloufi and N. Kezibri, Large-scale decomposition of green ammonia for pure hydrogen production, *Int. J. Hydrogen Energy*, 2021, **46**(70), 34777–34787.
42 J. Andersson and S. Grönkvist, Large-scale storage of hydrogen, *Int. J. Hydrogen Energy*, 2019, **44**(23), 11901–11919.
43 P. T. Aakko-Saksa, C. Cook, J. Kiviaho and T. Repo, Liquid organic hydrogen carriers for transportation and storing of renewable energy – Review and discussion, *J. Power Sources*, 2018, **396**, 803–823.
44 IRENA, *Global hydrogen trade to meet the 1.5 °C climate goal: Part II – Technology review of hydrogen carriers*, International Renewable Energy Agency, Abu Dhabi, 2022.
45 M. Fecke, S. Garner and B. Cox, Review of Global Regulations for Anhydrous Ammonia Production, Use, and Storage, *Hazards 26*, 2016, **161**, 11.
46 *GPSA Engineering Data book*, 14th edn.
47 E. Spatolisano, L. A. Pellegrini, A. R. de Angelis, S. Cattaneo and E. Roccaro, Ammonia as a Carbon-Free Energy Carrier:NH_3 Cracking to H_2, *Ind. Eng. Chem. Res.*, 2023, **62**, 10813–10827.
48 S. Ecuity, Engie and Siemens, Ammonia to Green Hydrogen Project, *Feasibility Study*, 2020, 1.
49 https://www.protonventures.com/news (accessed April 4, 2023).
50 https://www.uniper.energy/news/uniper-plans-to-makewilhelmshaven-a-hub-for-climate-friendly-hydrogen (accessed April 4, 2023).

51 W. M. Vatavuk, A review of ''PLANT DESIGN AND ECONOMICS FOR CHEMICAL ENGINEERS'' by Max S. Peters and Klaus D. Timmerhaus, McGraw-Hill, New York, 1980, 973 pages, list $26.00, *Eng. Economist.*, 1981, **27**(1), 90–93.
52 J. Ashcroft and H. Goddin, Centralised and Localised Hydrogen Generation by Ammonia Decomposition: a technical review of the ammonia cracking process, *Johnson Matthey Technol. Rev.*, 2022, **66**(4), 375–385.
53 R. Nasharuddin, M. Zhu, Z. Zhang and D. Zhang, A technoeconomic analysis of centralised and distributed processes of ammonia dissociation to hydrogen for fuel cell vehicle applications, *Int. J. Hydrogen Energy*, 2019, **44**(28), 14445–14455.
54 M. Asif, S. Sidra Bibi, S. Ahmed, M. Irshad, M. Shakir Hussain and H. Zeb, *et al.*, Recent advances in green hydrogen production, storage and commercial-scale use via catalytic ammonia cracking, *Chem. Eng. J.*, 2023, **473**, 145381.
55 I. Lucentini, X. Garcia, X. Vendrell and J. Llorca, Review of the Decomposition of Ammonia to Generate Hydrogen, *Ind. Eng. Chem. Res.*, 2021, **60**(51), 18560–18611.
56 D. A. Shlyapin, V. A. Borisov, V. L. Temerev, K. N. Iost, Z. A. Fedorova and P. V. Snytnikov, Ammonia Synthesis and Decomposition in the Presence of Supported Ruthenium Catalysts, *Kinet. Catal.*, 2023, **64**(6), 815–825.
57 T. Su, B. Guan, J. Zhou, C. Zheng, J. Guo and J. Chen, *et al.*, Review on Ru-Based and Ni-Based Catalysts for Ammonia Decomposition: Research Status, Reaction Mechanism, and Perspectives, *Energy Fuels*, 2023, **37**(12), 8099–8127.
58 K. Zheng, Y. Yan, Y. Sun, J. Yang, M. Zhu and M. Ni, *et al.*, An experimental study of ammonia decomposition rates over cheap metal catalysts for solid oxide fuel cell anode, *Int. J. Hydrogen Energy*, 2023, **48**(50), 19188–19195.
59 B. Lu, L. Li, M. Ren, Y. Liu, Y. Zhang and X. Xu, *et al.*, Ammonia decomposition over iron-based catalyst: exploring the hidden active phase, *Appl. Catal., B*, 2022, **314**, 121475.
60 T. E. T.-M. L. Bell, H_2 Production via Ammonia Decomposition Using Non-Noble Metal Catalysts: A Review, *Top. Catal.*, 2016, **59**(15–16), 1438–1457.
61 J. Łuczak and L. Torrente-Murciano, Nickel-based catalysts for electrolytic decomposition of ammonia towards hydrogen production, *Adv. Colloid Interface Sci.*, 2023, **319**, 102963.
62 T. An Le, Q. Cuong Do, Y. Kim, T.-W. Kim and H.-J. Chae, A review on the recent developments of ruthenium and nickel catalysts for COx-free H_2 generation by ammonia decomposition, *Korean J. Chem. Eng.*, 2021, **38**(6), 1087–1103.
63 Y. Im, H. Muroyama, T. Matsui and K. Eguchi, Ammonia decomposition over nickel catalysts supported on alkaline earth metal aluminate for H_2 production, *Int. J. Hydrogen Energy*, 2020, **45**(51), 26979–26988.
64 S. Sun, Q. Jiang, D. Zhao, T. Cao, H. Sha and C. Zhang, *et al.*, Ammonia as hydrogen carrier: advances in ammonia decomposition catalysts for promising hydrogen production, *Renewable Sustainable Energy Rev.*, 2022, **169**, 112918.
65 Z. Su, J. Guan, Y. Liu, D. Shi, Q. Wu and K. Chen, *et al.*, Research progress of ruthenium-based catalysts for hydrogen production from ammonia decomposition, *Int. J. Hydrogen Energy*, 2024, **51**, 1019–1043.
66 T. J. Wood and J. W. Makepeace, Assessing Potential Supports for Lithium Amide-imide Ammonia Decomposition Catalysts, *ACS Appl. Energy Mater.*, 2018, **1**(6), 2657–2663.
67 J. W. Makepeace, H. M. A. Hunter, T. J. Wood, R. I. Smith, C. A. Murray and W. I. F. David, Ammonia decomposition catalysis using lithium-calcium imide, *Faraday Discuss.*, 2016, **188**, 525–544.
68 J. W. Makepeace, T. J. Wood, H. M. A. Hunter, M. O. Jones and W. I. F. David, Ammonia decomposition catalysis using non-stoichiometric lithium imide, *Chem. Sci.*, 2015, **6**(7), 3805–3815.
69 J. W. Makepeace, T. J. Wood, P. L. Marks, R. I. Smith, C. A. Murray and W. I. F. David, Bulk phase behavior of lithium imide-metal nitride ammonia decomposition catalysts. Physical chemistry chemical physics, *Phys. Chem. Chem. Phys.*, 2018, **20**(35), 22689–22697.
70 H. M. A. Hunter, J. W. Makepeace, T. J. Wood, O. S. Mylius, M. G. Kibble and J. B. Nutter, *et al.*, Demonstrating hydrogen production from ammonia using lithium imide – Powering a small proton exchange membrane fuel cell, *J. Power Sources*, 2016, **329**, 138–147.
71 W. I. F. David, J. W. Makepeace, S. K. Callear, H. M. A. Hunter, J. D. Taylor and T. J. Wood, *et al.*, Hydrogen Production from Ammonia Using Sodium Amide, *J. Am. Chem. Soc.*, 2014, **136**(38), 13082–13085.
72 M. Yang, U. Raucci and M. Parrinello, Reactant-induced dynamics of lithium imide surfaces during the ammonia decomposition process, *Nat. Catal.*, 2023, **6**(9), 829–836.
73 I. Lucentini, X. Garcia, X. Vendrell and J. Llorca, Review of the Decomposition of Ammonia to Generate Hydrogen, *Ind. Eng. Chem. Res.*, 2021, **60**(51), 18560–18611.
74 E. P. Perman, G. A. S. Atkinson and W. Ramsay, The decomposition of ammonia by heat, *Proc. R. Soc. London*, 1905, **74**(497), 110–117.
75 C. Tyler, Ammonia as a source of hydrogen for hardening oils, *J. Am. Oil Chem. Soc.*, 1934, **11**(11), 231.
76 S. Devkota, J.-Y. Cha, B.-J. Shin, J.-H. Mun, H. C. Yoon and S. A. Mazari, *et al.*, Techno-economic and environmental assessment of hydrogen production through ammonia decomposition, *Appl. Energy*, 2024, **358**, 122605.
77 G. E. Pitselis, P. D. Petrolekas and C. G. Vayenas, Electrochemical promotion of ammonia decomposition over Fe catalyst films interfaced with K + - & H + — conductors, *Ionics*, 1997, **3**(1–2), 110–116.
78 G. Marnellos, S. Zisekas and M. Stoukides, Synthesis of Ammonia at Atmospheric Pressure with the Use of Solid State Proton Conductors, *J. Catal.*, 2000, **193**(1), 80–87.
79 S. Zisekas, G. Karagiannakis, G. Marnellos and M. Stoukides, Study of ammonia decomposition in a proton conducting solid electrolyte cell, *Ionics*, 2002, **8**(1–2), 118–122.

80 C. Smith and H. Essex, Effect of Electric Fields on the Decomposition of Ammonia by Alpha-Rays, *J. Chem. Phys.*, 1938, **6**(4), 188–196.
81 Y. Zhao, L. Wang, J. Zhang, W. Gong and H. Guo, Decomposition of ammonia by atmospheric pressure AC discharge: catalytic effect of the electrodes, *Catal. Today*, 2013, **211**, 72–77.
82 J. Lee, S. Ga, D. Lim, S. Lee, H. Cho and J. Kim, Carbon-free green hydrogen production process with induction heating-based ammonia decomposition reactor, *Chem. Eng. J.*, 2023, **457**, 141203.
83 Y. Yi, L. Wang, Y. Guo, S. Sun and H. Guo, Plasma-assisted ammonia decomposition over Fe–Ni alloy catalysts for COx-Free hydrogen, *AIChE J.*, 2019, **65**(2), 691.
84 Y. Hayakawa, T. Miura, K. Shizuya, S. Wakazono, K. Tokunaga and S. Kambara, Hydrogen production system combined with a catalytic reactor and a plasma membrane reactor from ammonia, *Int. J. Hydrogen Energy*, 2019, **44**(20), 9987–9993.
85 M. Akiyama, K. Aihara, T. Sawaguchi, M. Matsukata and M. Iwamoto, Ammonia decomposition to clean hydrogen using non-thermal atmospheric-pressure plasma, *Int. J. Hydrogen Energy*, 2018, **43**(31), 14493–14497.
86 T. Hu and Y. Wang, Effect of Operating and Geometrical Parameters on Ammonia Decomposition in a Tubular Reactor Driven by Concentrating Solar Power, *J. Energy Eng.*, 2020, **146**(4), DOI: **10.1061/(ASCE)EY.1943-7897.0000664**.
87 B. Wang, H. Kong, H. Wang, Y. Wang and X. Hu, Kinetic and thermodynamic analyses of mid/low-temperature ammonia decomposition in solar-driven hydrogen permeation membrane reactor, *Int. J. Hydrogen Energy*, 2019, **44**(49), 26874–26887.
88 N. Engelbrecht, S. Chiuta and D. G. Bessarabov, A highly efficient autothermal microchannel reactor for ammonia decomposition: analysis of hydrogen production in transient and steady-state regimes, *J. Power Sources*, 2018, **386**, 47–55.
89 S. Chiuta and D. G. Bessarabov, Design and operation of an ammonia-fueled microchannel reactor for autothermal hydrogen production, *Catal. Today*, 2018, **310**, 187–194.
90 P. Modisha and D. Bessarabov, Nitrogen Compounds, Researchers from North West University Report Recent Findings in Nitrogen Compounds (Electrocatalytic Process for Ammonia Electrolysis: A Remediation Technique with Hydrogen Co-Generation), *Int. J. Electrochem. Sci.*, 2016, DOI: **10.20964/2016.08.54**.
91 A. Iwase, K. Li and A. Kudo, Decomposition of an aqueous ammonia solution as a photon energy conversion reaction using a Ru-loaded ZnS photocatalyst, *Chem. Commun.*, 2018, **54**(48), 6117–6119.
92 M. Reli, N. Ambrožová, M. Šihor, L. Matějová, L. Čapek and L. Obalová, *et al.*, Novel cerium doped titania catalysts for photocatalytic decomposition of ammonia, *Appl. Catal., B*, 2015, **178**, 108–116.
93 Q. Xia, Z. Lin, C. Wang, Z. Pan, W. Jin and C. Chen, *et al.*, Solar-driven multichannel membrane reactor for hydrogen production from ammonia decomposition, *Fuel*, 2024, **356**, 129591.
94 V. Cechetto, S. Agnolin, L. Di Felice, A. Pacheco Tanaka, M. Llosa Tanco and F. Gallucci, Metallic Supported Pd–Ag Membranes for Simultaneous Ammonia Decomposition and H_2 Separation in a Membrane Reactor: Experimental Proof of Concept, *Catalysts*, 2023, **13**(6), 920.
95 R. Sitar, J. Shah, Z. Zhang, H. Wikoff, J. D. Way and C. A. Wolden, Compact ammonia reforming at low temperature using catalytic membrane reactors, *J. Membr. Sci.*, 2022, **644**(C), 120147.
96 J. Liu, X. Ju, C. Tang, L. Liu, H. Li and P. Chen, High performance stainless-steel supported Pd membranes with a finger-like and gap structure and its application in NH_3 decomposition membrane reactor, *Chem. Eng. J.*, 2020, **388**, 124245.
97 V. Cechetto, L. Di Felice, R. Gutierrez Martinez, A. Arratibel Plazaola and F. Gallucci, Ultra-pure hydrogen production via ammonia decomposition in a catalytic membrane reactor, *Int. J. Hydrogen Energy*, 2022, **47**(49), 21220–21230.
98 S. Devkota, B.-J. Shin, J.-H. Mun, T.-H. Kang, H. C. Yoon and S. A. Mazari, *et al.*, Process design and optimization of onsite hydrogen production from ammonia: reactor design, energy saving and NOX control, *Fuel*, 2023, **342**, 127879.
99 J. H. Kim, H. U. Um and O. C. Kwon, Hydrogen production from burning and reforming of ammonia in amicroreforming system, *Energy Convers. Manage.*, 2012, **56**, 184–191.
100 V. Cechetto, L. Di Felice, J. A. Medrano, C. Makhloufi, J. Zuniga and F. Gallucci, H_2 production via ammonia decomposition in a catalytic membrane reactor, *Fuel Process. Technol.*, 2021, **216**, 106772.
101 R. Ao, R. Lu, G. Leng, Y. Zhu, F. Yan and Q. Yu, A Review on Numerical Simulation of Hydrogen Production from Ammonia Decomposition, *Energies*, 2023, **16**(2), 921.
102 Institute GC. GCCSI. Global CCS Institute – toward a common method of cost estimation for CO_2 capture and storage at fossil fuel power plants. 2013. 2013.
103 S. M. Nazir, J. Hendrik Cloete, S. Cloete and S. Amini, Pathways to low-cost clean hydrogen production with gas switching reforming, *Int. J. Hydrogen Energy*, 2021, **46**(38), 20142–20158.
104 Y. Yan, V. Manovic, E. J. Anthony and P. T. Clough, Techno-economic analysis of low-carbon hydrogen production by sorption enhanced steam methane reforming (SE-SMR) processes, *Energy Convers. Manage.*, 2020, **226**, 113530.
105 H. P. Loh, Energy USDo, National Energy Technology Laboratory & Jennifer Lyons and Charles W. White I, EG&G Technical Services I. Process Equipment Cost Estimation Final Report, DOE/NETL-2002/1169 2002.
106 Laboratory NET. National Energy Technology Laboratory, Assessment of hydrogen Production with CO_2 Capture Volume 1: Baseline-State-Of the Arts Plant, Revision 1, Nov 14th, 2011, DOE/NETL-2011/1434. 2011.

107 M. Bozorg, B. Addis, V. Piccialli, Á. A. Ramírez-Santos, C. Castel and I. Pinnau, *et al.*, Polymeric membrane materials for nitrogen production from air: a process synthesis study, *Chem. Eng. Sci.*, 2019, **207**, 1196–1213.
108 A. Di Carlo, L. Vecchione and Z. Del Prete, Ammonia decomposition over commercial Ru/Al_2O_3 catalyst: an experimental evaluation at different operative pressures and temperatures, *Int. J. Hydrogen Energy*, 2014, **39**(2), 808–814.
109 S. Richard, A. Ramirez Santos, P. Olivier and F. Gallucci, Techno-economic analysis of ammonia cracking for large scale power generation, *Int. J. Hydrogen Energy*, 2024, **71**, 571–587.